Mechanistic insights into allosteric PKR activation guide design of a clinical-stage allosteric agonist

Haiyun Ma[1,2], Quanwei Yu[1], Ling Zhang[3], Xiao Hu[3], Zao Wang[3], Jing Wang[3], Jun Tang[3], Zhaoming Su[1,*]

[1]Center of Infectious Diseases, State Key Laboratory of Biotherapy and Biosafety Laboratory, Institute of Infection and Infectious Diseases, West China Hospital, Sichuan University, Chengdu 610044, China.

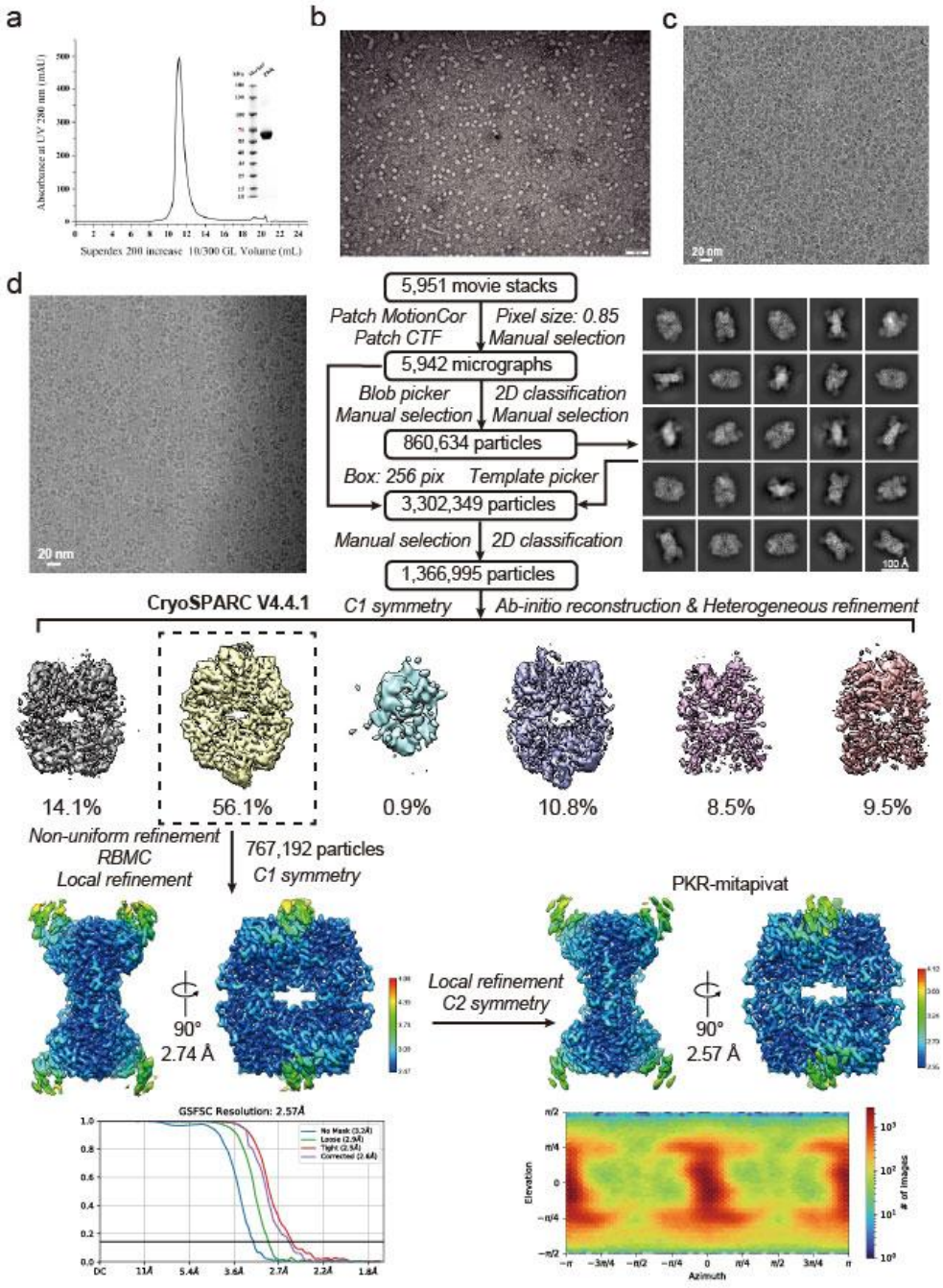
[2]Tianfu Jincheng Laboratory, Chengdu, 610093, China.

[3]ScinnoHub Pharmaceutical Co., Ltd, No. 263 Hexiang Third Street, Shuangliu District, Chengdu, 610000, China

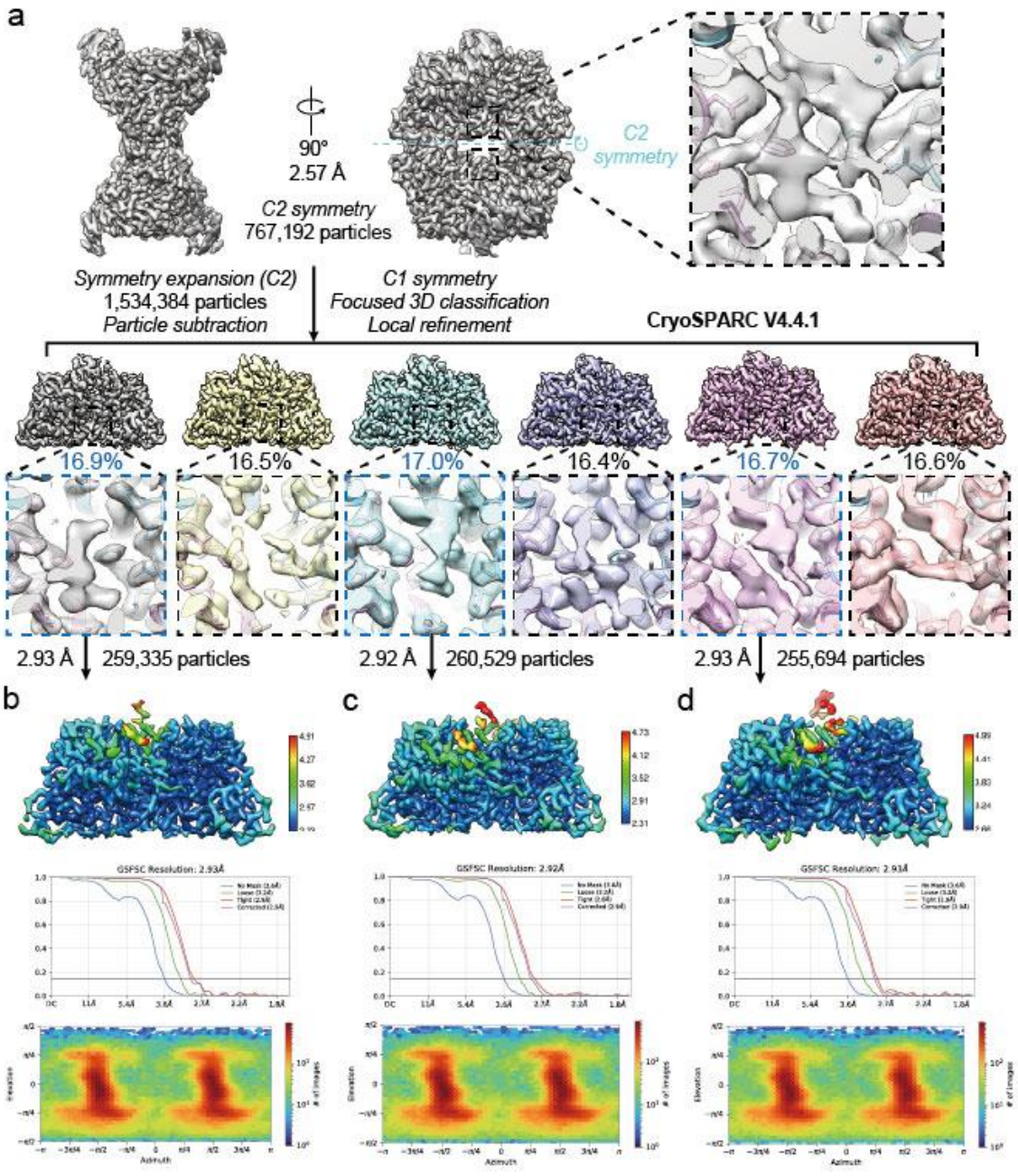
*Correspondence should be addressed to Z.S. (zsu@wchscu.cn).

This file includes:

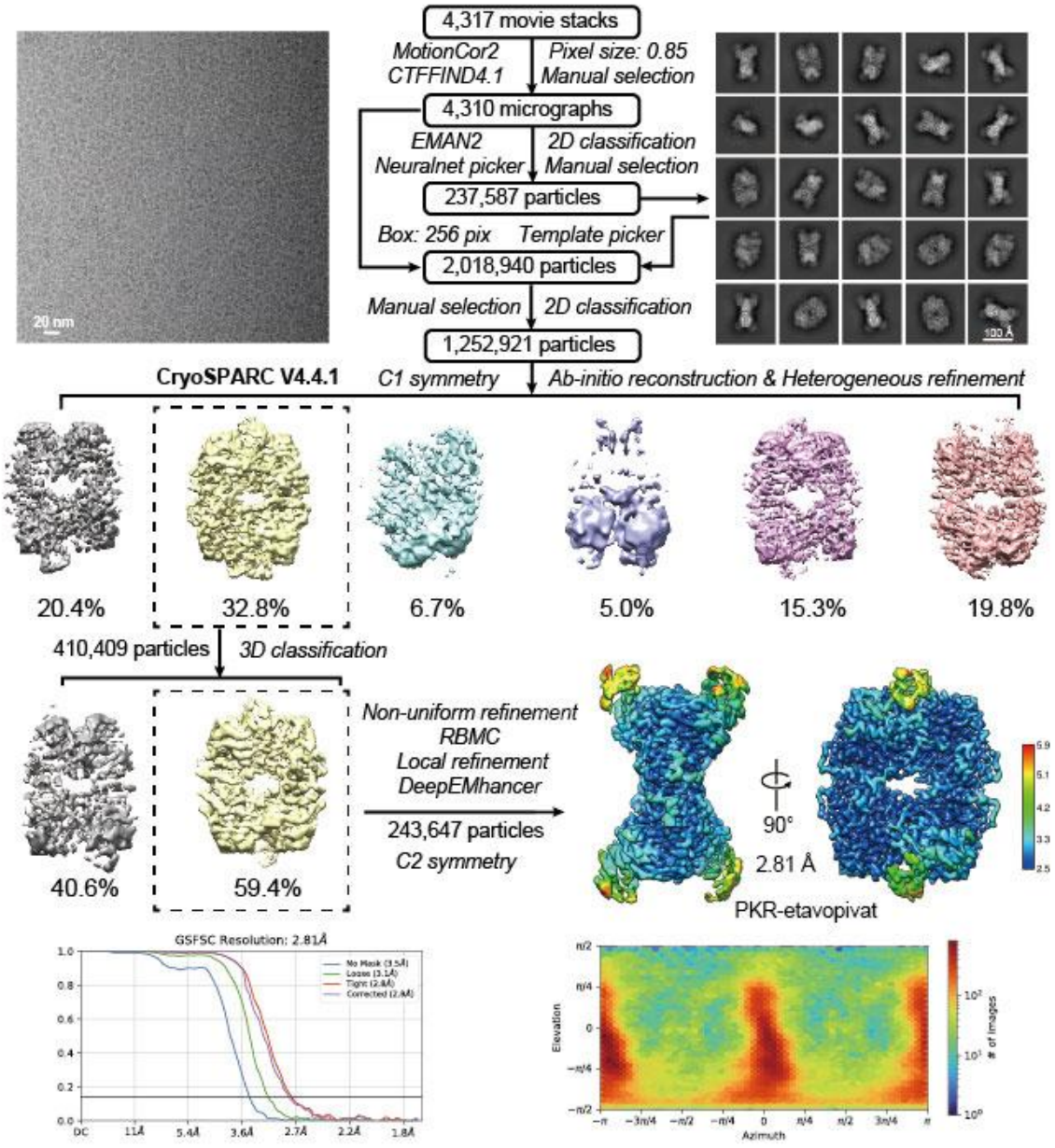
Extended Data Figs. 1 to 6



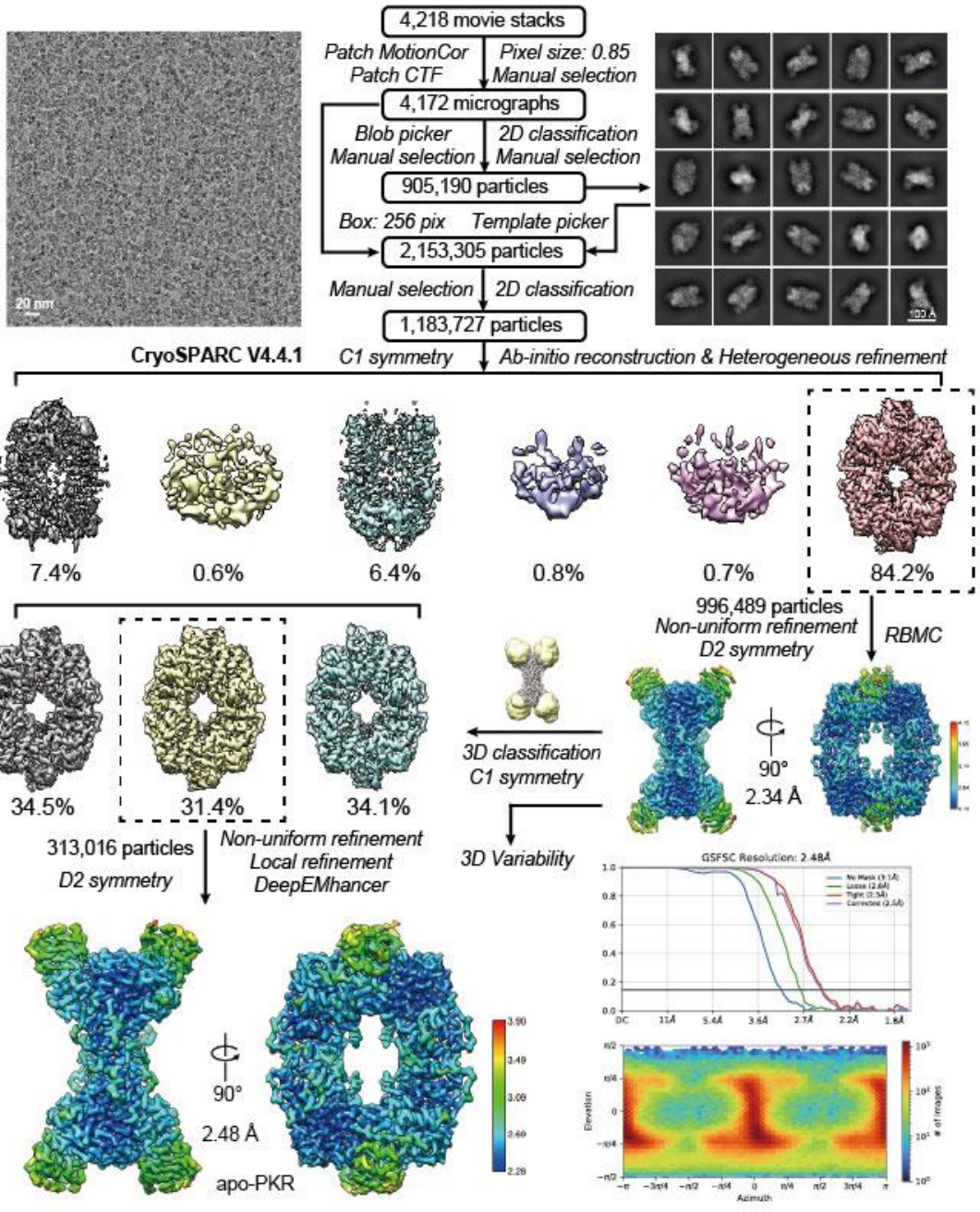
Extended Data Fig. 1 | Purification of PKR and cryo-EM processing of the PKR-mitapivat complex. a, Size-exclusion chromatography and SDS-PAGE analysis of purified full-length human PKR. b, Representative negative-stain micrograph of PKR. c, Representative cryo-EM image of PKR showing well-dispersed particles. d, Cryo-EM workflow for the PKR-mitapivat complex, including 2D class averages, 3D classification, 3D reconstruction at 2.74 Å resolution in C1 and at 2.57 Å resolution after C2 local refinement, FSC curve and particle orientation distribution. The same 767,192-particle set was used for the symmetry expansion and focused classification shown in Extended Data Fig. 2. Related to Figure 1.



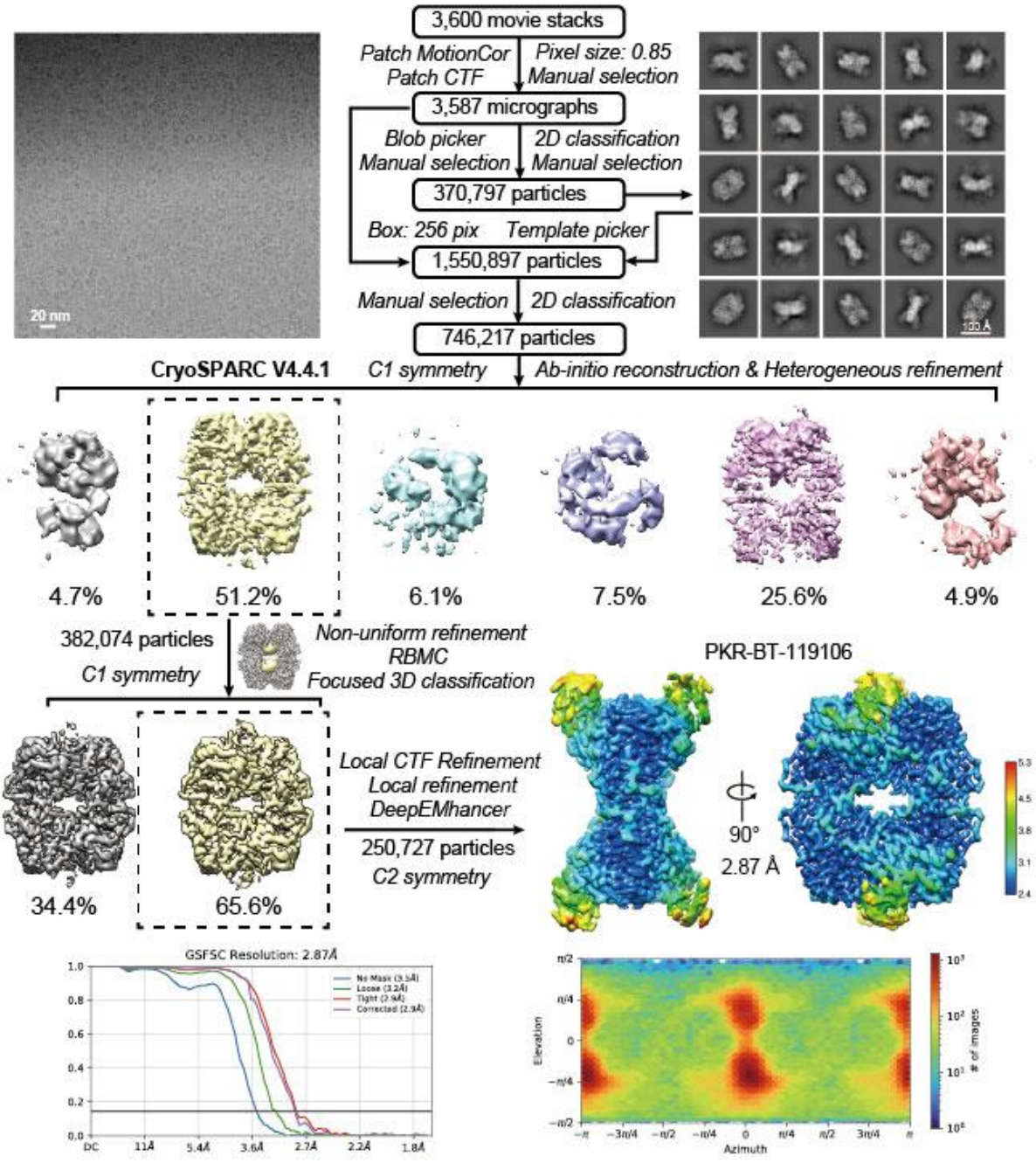
Extended Data Fig. 2 | Focused classification of the PKR-mitapivat complex resolves one dual-ligand and two single-ligand states. a, C2 symmetry expansion of the 767,192-particle set from Extended Data Fig. 1, followed by signal subtraction and focused 3D classification without imposed symmetry, yielded six classes. b-d, The three classes with explicit ligand density were independently refined to 2.9 Å resolution, corresponding to single-ligand pose A (b), single-ligand pose B (c) and the dual-ligand state (d). Each panel includes the final map colored by local resolution, the FSC curve and the particle orientation distribution. Related to Figure 1c.



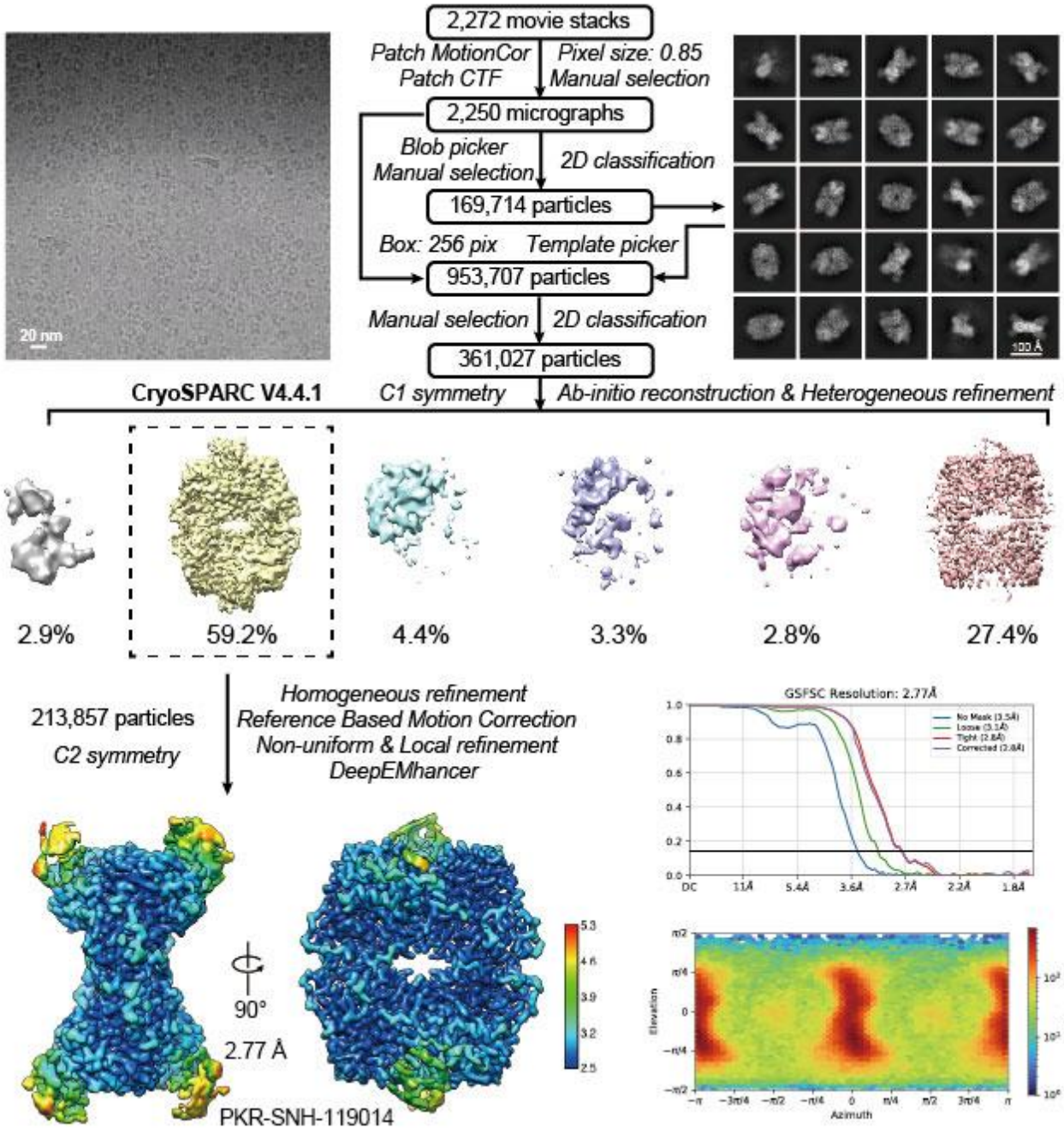
Extended Data Fig. 3 | Cryo-EM workflow for the PKR-etavopivat complex. Of 4,317 movie stacks, 4,310 micrographs were selected and 1,252,921 particles were retained after 2D classification, and two rounds of 3D classification yielded a final set of 243,647 particles that reconstructed the map at 2.81 Å resolution with C2 symmetry. The workflow includes representative micrograph and 2D averages, 3D classification, 3D reconstruction, FSC curve and particle orientation distribution. Related to Figure 2.



Extended Data Fig. 4 | Cryo-EM workflow for apo-PKR. Of 4,218 movie stacks, 4,172 micrographs were selected and 1,183,727 particles were retained after 2D classification, and heterogeneous refinement yielded 996,489 particles that reconstructed the consensus map at 2.34 Å resolution with D2 symmetry. Focused 3D classification of the B domain without imposed symmetry separated three classes, and refinement of the intermediate class containing 313,016 particles with D2 symmetry reconstructed the map at 2.48 Å resolution. Three-dimensional variability analysis was performed on the 996,489-particle set. The workflow includes representative micrograph and 2D averages, 3D classification, 3D reconstruction, FSC curves and particle orientation distributions. Related to Figure 3a.



Extended Data Fig. 5 | Cryo-EM workflow for the PKR-BT-119106 complex. Of 3,600 movie stacks, 3,587 micrographs were selected and 746,217 particles were retained after 2D classification, heterogeneous refinement selected 382,074 particles, and focused 3D classification of the interfacial allosteric pocket yielded a final set of 250,727 particles that reconstructed the map at 2.87 Å resolution with C2 symmetry. The workflow includes representative micrograph and 2D averages, 3D classification, 3D reconstruction, FSC curve and particle orientation distribution. Related to Figure 5a-c.



Extended Data Fig. 6 | Cryo-EM workflow for the PKR-SNH-119014 complex. Of 2,272 movie stacks, 2,250 micrographs were selected and 361,027 particles were retained after 2D classification, and heterogeneous refinement yielded a final set of 213,857 particles that reconstructed the map at 2.77 Å resolution with C2 symmetry. The workflow includes representative micrograph and 2D averages, 3D classification, 3D reconstruction, FSC curve and particle orientation distribution. Related to Figure 5d-f.